AIAA JOURNAL
Vol. 42, No. 7, July 2004

Low-Frequency Modulations Associated with Vortex Shedding from Flow over Bluff Body

J. J. Miau,* S. J. Wu,† C. C. Hu,‡ and J. H. Chou§
National Cheng-Kung University, Tainan 70101, Taiwan, Republic of China

The characteristic behaviors of low-frequency modulations embedded in the vortex shedding process behind a trapezoidal cylinder were studied experimentally. Hot-wire signals and smoke-wire visualization images were acquired simultaneously to examine the correlation between low-frequency modulations and the vortex formation length. Wavelet analysis was performed to extract the instantaneous properties from the raw hot-wire signals measured upstream of the trapezoidal cylinder model. Results show that the variations of instantaneous vortex shedding frequency appear to be in negative correlation with the low-frequency modulations and that the cross-correlation coefficient can reach −0.5. This substantiates that the low-frequency modulations observed are linked with the vortex shedding process.

I. Introduction

FLOW around a cylindrical bluff body involves the phenomena of boundary-layer separation, free shear layer, and wake development, which have been studied for decades. It is well known that the phenomenon of periodic vortex shedding occurs at sufficiently high Reynolds numbers. On the other hand, researchers also noticed that amplitudes of velocity and pressure fluctuations measured in the vortex shedding process appear to contain modulations whose timescale is significantly larger than the shedding period. This phenomenon is referred to as the low-frequency modulation or unsteadiness in many reports, and it has been observed with different configurations of bluff bodies in different ranges of Reynolds numbers.

Some of the earliest works concerning the low-frequency behavior of vortex shedding behind a bluff body include those of Roshko,[1] Tritton,[2] Bloor,[3] Gerrard,[4] and Hanson and Richardson.[5] Since then, a number of observations and interpretations were reported in the literature, and many of them linked the low-frequency fluctuations to the three-dimensional characteristics of the vortex shedding structures. Roshko[6] attributed the three dimensionality of wake flows to the extrinsic and intrinsic effects. The extrinsic effects experimentally observed are often related to the aspect ratio of a bluff body as reported by Graham,[7] Fox and West,[8] Szepessy and Bearman,[9] and Norberg.[10] Discussions on the arrangement of end plates can be seen in Refs. 11–13. On the other hand, the intrinsic characteristics of three dimensionality can be found in the experimental results by Williamson,[14,15] Yang et al.,[16] and Blackburn and Melbourne,[17] and on the numerical results by Henderson[18] and Najjar and Balachandar.[19] Lisoski[20] suggested that in reality, both of the extrinsic and intrinsic effects be present in a wake flow. Further detailed review on the papers just mentioned can be found in Ref. 21.

In studying the relation between the variations of vortex shedding frequency and the modulations of signal amplitude, Gerrard[4] found that, in the stable range ($Re = 85$), the modulation of the hot-wire signal is directly related to the difference in the vortex shedding frequencies measured, and the modulation is a result of flapping of the wake. In the transition range ($Re = 235$), the relation found at $Re = 85$, of maximum modulation coupled with minimum period, is only roughly true. In the turbulent range ($Re = 2 \times 10^4$), no evidence available concerning the flapping of the wake or the correlation between modulation of the signal amplitude and the shedding periods has been reported. Analyzing the signals measured by the flush-mounted thermal films on a circular cylinder at Reynolds numbers from 2×10^4 to 4×10^4, Blevins[22] pointed out that the vortex shedding process is a series of coherent strings of events whose frequencies wander 1–2% about the nominal vortex-shedding frequency. He also found that there is a tendency for the larger amplitude to have lower frequency. However, in the literature, there is a lack of quantitative and instantaneous information describing the relation between the vortex-shedding frequency and low-frequency modulation.

The present work was motivated by an earlier study on the quality of the vortex shedding signals for a vortex flowmeter. As noted by Miau et al.,[23] the pressure fluctuations measured on the surface of a trapezoidal cylinder installed in a circular pipe contained a substantial component of low-frequency variations for the Reynolds numbers were larger than 10^3, and the low-frequency variations are associated with the unsteady variations of the vortex formation length. Later, Miau et al.[24] performed experiments with a trapezoidal cylinder and a circular cylinder, respectively, to examine the relation between the low-frequency variations embedded in the base pressure signals and the velocity signals measured in the near wake region. The results of both cases showed that the unsteady variations of the vortex formation length and base pressure are closely related in a real-time manner. As the base pressure is increased, the vortex formation region is lengthened, and vice versa. Recently, Miau et al.[21] defined an optimal cutoff frequency for the purpose of extracting the low-frequency fluctuations in the near wake region of a trapezoidal cylinder. The integral timescale of the low-pass fluctuations in reference to the optimal cutoff frequency was found to be about two times the vortex-shedding period. Miau et al.[21] also found that the low-frequency fluctuations in the near wake region exhibit a global characteristic, which could be linked to the spanwise motions of the separated shear layer.

The present work aims to identify the linkage between the low-frequency modulations and the instantaneous vortex-shedding frequency measured for flow over a bluff body. At first, the hot-wire measurements and the smoke-wire visualization were conducted simultaneously to reveal the relation between the low-frequency variations and vortex formation length. Second, the linkage between the low-frequency modulations and the instantaneous vortex-shedding frequency reduced by wavelet analysis was examined with a cross-correlation method. Finally, the integral timescale of the low-frequency component was deduced for further comparison with previous findings.[21]

Presented as Paper 2003-1122 at the 41st Aerospace Sciences Meeting, Reno, NV, 6–9 January 2003; received 31 March 2003; revision received 21 November 2003; accepted for publication 10 February 2004.

*Professor, Department of Aeronautics and Astronautics. Associate Fellow AIAA.
†Graduate Student, Department of Aeronautics and Astronautics.
‡Postdoctor, Department of Aeronautics and Astronautics.
§Professor, Department of Engineering Science.

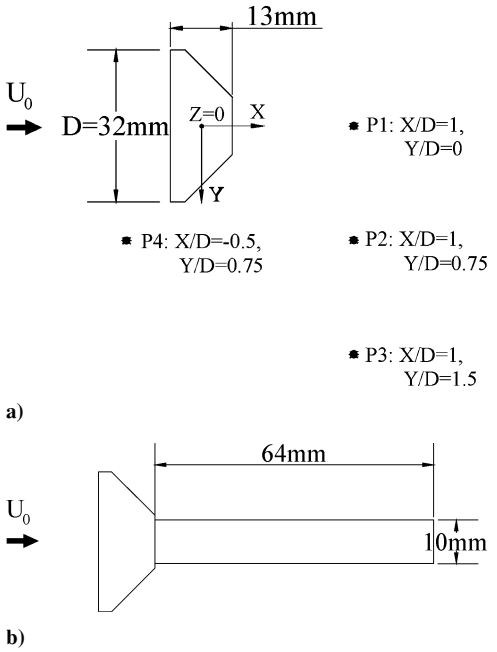

Fig. 1 Trapezoidal cylinder a) and the positions of hot-wire measurements and b) with splitter plate.

II. Experimental Method

A closed-return low-speed wind tunnel was employed for the present study. The test section was 150 mm × 150 mm in cross section. Turbulence intensity measured at the centerline of the test section was less than 1%, based on the mean velocity U_0 in a range between 2 and 20 m/s. Efforts were made to verify that no peculiar fluctuating components were present in the freestream flow, and the nonuniformity of the mean flow in the test section, excluding the boundary-layer regions along the walls, was less than 0.5% of the mean velocity measured.

A trapezoidal cylinder was employed as the bluff body, with its maximum width facing the incoming flow. The width, denoted as D, was 32 mm. Based on D, the blockage ratio was about 21%. As the trapezoidal cylinder was spanned between the two sidewalls, the aspect ratio of the cylinder, that is, the spanwise length of the cylinder vs D, was 4.7. Figure 1a shows a cross-sectional view of the trapezoidal cylinder at the midspan. Furthermore, a 10-mm-thick splitter plate of $2D$ in length could be placed at the rear end of the trapezoidal cylinder, shown in Fig. 1b. The addition of this splitter plate for comparison was motivated by an earlier finding[23] that the low-frequency variations in the vortex-shedding signals measured could be successfully suppressed if a splitter plate attached behind the trapezoidal cylinder was $2D$ long. Based on D and U_0, the Reynolds numbers Re were 1.8×10^3 for the smoke-wire flow visualization experiments and up to 2.7×10^4 for the hot-wire measurements.

The coordinate system employed for the present study is also indicated in Fig. 1a. X denotes the streamwise axis pointing downstream, and $X = 0$ is located at 6.5 mm downstream of the frontal face of the trapezoidal cylinder. Y denotes the vertical axis, and $Y = 0$ is coincided with the centerline of the test section. Z denotes the spanwise axis, and $Z = 0$ is located at the midspan of the cylinder.

Vortex-shedding signals were obtained by a single hot-wire probe, Dantec 55P11. Moreover, a smoke-wire flow visualization technique was employed to reveal the shedding vortical structures. With an electronic trigger device, the data acquisition system and the charge-coupled device (CCD) camera for flow visualization could work in a synchronous manner.

III. Wavelet Analysis

Wavelet transform (WT) is a mathematical tool pertinent to the study of the nonstationary signal. After Grossman and Morlet,[25] WT has been applied to a range of fields in science. Some applications of WT in wake flow studies are briefly reviewed as follows. Kiya and Abe[26] plotted the time history of the fluctuating part of modulus of wavelet coefficient at the scale of vortex shedding and then obtained the representative frequency of the low-frequency unsteadiness. Lewis and Gharib[27] implemented a local frequency analysis concerning the wavelet coefficient at the scale of vortex-shedding structures to explore the frequency modulations in the wake. Hangan et al.[28] developed a wavelet pattern recognition technique (WPR) to identify the primary and secondary structures of cylinder wakes. Higuchi et al.[29] employed conditional spectra to study the evolution of the vortex patterns in the wake behind a pair of flat plates. On vortex dislocations in three-dimensional wake transition, Braza et al.[30] conducted a numerical study with wavelet analysis and autoregressive modeling of the time series. More papers on wavelet analysis with turbulent flows can be found in Ref. 31.

In the present study, the instantaneous properties, including vortex-shedding frequency and amplitude modulation, were of interest and obtained by WT. On the other hand, it was clear that the most direct method for determination of instantaneous frequency is the Hilbert transform (HT) (see Ref. 32). Recently, Hu et al.[33] successfully employed the empirical mode decomposition method (EMD) developed by Huang et al.[34] and applied HT to obtain the instantaneous vortex-shedding frequency of the velocity signals in a periodically varying flow. However it was realized that, if the raw signal comprised intermittent fluctuations, the EMD technique could not be applied straightforwardly.[34] In the present study, WT was chosen because the vortex-shedding signals measured contained noiselike fluctuations.

WT of a signal $g(t)$ with respect to a wavelet $\psi(t)$ is defined by a convolution integral[25]:

$$W(a,b) = \frac{1}{\sqrt{a}} \int g(t)\psi^*\left(\frac{t-b}{a}\right) \mathrm{d}t \tag{1}$$

where a denotes the scale, b denotes the translation, and ψ^* is the complex conjugate of ψ. In this work, the continuous Morlet wavelet, given hereafter, was employed for WT:

$$\psi(T) = e^{ik_\psi T} e^{-T^2/2} \tag{2}$$

where the parameter k_ψ was taken to be 6.0 to satisfy the admissibility condition.[31] The selection of Morlet wavelet was based on the following considerations: a) to yield the most detailed multiscale structure of the velocity fluctuations[35] and b) to give the satisfactory performance for the present signals measured.[36] After the wavelet function and the relative parameters were chosen, the computation according to Eq. (1) could be carried out. Then, the wavelet coefficient $W(a,b)$ in Eq. (1) could be transformed analytically into $W(f,t)$ (Ref. 37), where f and t are frequency and time, respectively. Namely, the present wavelet analysis is capable of providing the modulus, $|W(f,t)|$, at a specific time and frequency with regard to the signal analyzed. The extraction of the instantaneous vortex shedding frequency via WT was based on the detection of ridges in the modulus of wavelet coefficients as follows[38]: 1) Find $f_{\max}$ at which the modulus $|W(f_{\max},t)|$ is the maximum. 2) Apply 1 to all t and adjoin $\{f_{\max}, t\}$ pairs to compose the instantaneous vortex-shedding frequency $f_w(t)$. On the other hand, the amplitude modulation $A_w(t)$, characterizing the low-frequency unsteadiness of vortex-shedding signal is defined as $|W(f_w(t),t)|$.

Note that because WT is based on the concept of Fourier transformation, large errors may occur at the beginning and end of the finite length time series. Following Torrence and Compo,[37] the cone of influence is the region of the wavelet spectrum where the edge effects become important. Thus, data inside the cone of influence were rejected before the correlation analysis applied.

IV. Results and Discussion

A. Low-Frequency Modulations Embedded in Hot-Wire Signals

Figure 2a shows the hot-wire traces obtained at $Re = 1.8 \times 10^3$ at four locations in the flowfield, whose coordinates are indicated

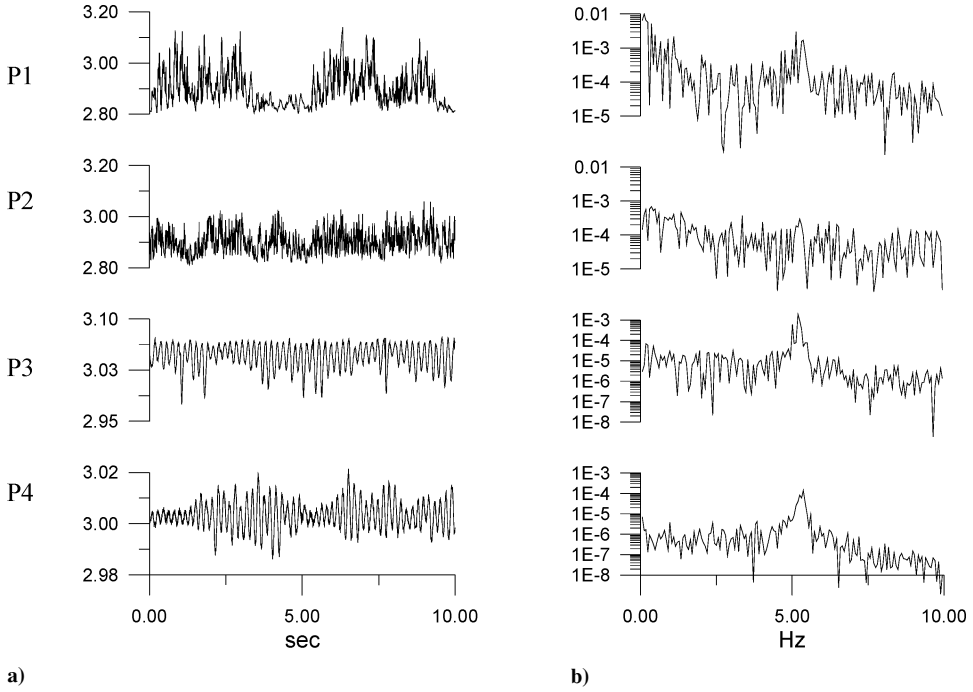

Fig. 2 Hot-wire measurements at points P1, P2, P3, and P4, respectively; $Re = 1.8 \times 10^3$: a) time traces and b) corresponding FFT spectra.

in Fig. 1. Figure 2b presents the corresponding frequency spectra. At point P1, in the near wake region, the hot-wire signals measured are dominated by irregular fluctuations, where the frequency component of vortex shedding can not be clearly identified. At point P2, which is located roughly at the inner edge of the shear layer, the hot-wire signals measured are dominated by the fluctuations at the vortex-shedding frequency; however, the amplitude varies significantly with time. This is explained by the shear-layer flapping; as the shear layer gets close to the measured point, the signals show, larger amplitude of fluctuations, and vice versa. Outside the wake shear layer (point P3) and upstream the model (point P4), the hot-wire signals measured are clearly characterized by the fluctuations at the vortex shedding frequency, together with low-frequency modulations. Based on the preceding observations, the signals obtained at points P3 and P4 are considered for further analysis and will be compared with the smoke-wire flow visualization images obtained.

Preliminary examinations confirmed that the low-frequency unsteadiness observed did not originate from the incoming flow. This will be shown hereafter. The signals of the model without and with a splitter plate are compared in Fig. 3, where both cases were measured at point P4, $Re = 4 \times 10^3$. Obviously, the appearance of low-frequency modulations is greatly suppressed in the case with the splitter plate. Similar findings were reported by Miau et al.[23] The wavelet spectra corresponding to these two cases are also presented in Fig. 3. In Fig. 3a, that is, the case without the splitter plate, the isovalue contours in the neighborhood of the shedding frequency appear in wavy patterns, in contrast to the flat appearance in Fig. 3b. Note that in Fig. 3b, the vortex-shedding frequency, corresponding to the maximum modulus at each time instant, appears to be rather constant. This comparison suggests that significant variations of the instantaneous vortex shedding in the case of Fig. 3a may be a result of the geometry of the bluff body. After this clarification, only the results of the model without the splitter plate will be presented and discussed in the following.

Figure 4 presents a segment of the hot-wire signals obtained at point P3 and the smoke-wire images of the wake flow structures. Note that, in this case, at $Re = 1.8 \times 10^3$, the vortex shedding frequency was 6.0 Hz, obtained from the frequency spectral analysis. The images shown were captured at a rate of 25 frames per second, hence, about four images were obtained within one shedding period.

The relation between the low-frequency modulations in shedding signals and the variations of the formation length can be realized from Fig. 4. As seen in Fig. 4a, the amplitude of hot-wire signal fluctuations in time zone 1 is comparatively larger than that in time zone 2. Also note that in Fig. 4c, the images corresponding to time zone 2 show the separated shear layer rolling up closer to the model, compared to the images corresponding to time zone 1, shown in Fig. 4b. Similar flow behavior can also be seen in Fig. 5, in which the hot-wire signals measured at point P4 and the smoke-wire images obtained simultaneously are presented for comparison.

With the smoke visualization photographs given in Figs. 4 and 5, further comments on a physical picture concerning the vortex formation region swollen-and-shrunk in time can be made as follows. As the separation region gets swollen, the separated shear layer rolls up farther away from the model; thus, the vortex formation length gets longer, and the amplitude of vortex shedding component in the hot-wire signals measured increases and vice versa. Moreover, the variations of the size of the separation region are associated with the base pressure fluctuations.[24] In Ref. 24, a correlation between the velocity signatures obtained by a split fiber and the base pressure measurements made on the bluff cylinder evidences that the unsteady variations of the vortex formation length and base pressure are closely related. To sum up, the unsteady phenomenon involved in the vortex-shedding process, understood from the preceding experimental observations, is featured with two timescales, one of which is associated with vortex shedding, and the other with the variations of the size of the vortex formation region. The latter appears to be of one order of magnitude larger than the former.

Note in Fig. 4 that low-frequency modulations associated with the hot-wire signals measured at point P3 cause significant variations in the short-time averaged dc level, which might distract from the present interest, for which the amplitude modulation associated with unsteady vortex shedding is of primary concern. Because of this concern, it is preferrable to employ the hot-wire signals measured at point P4, whose short-time averaged dc level is shown to be influenced less by the low-frequency modulations, for later analysis.

B. Correlation Between Low-Frequency Modulation and Vortex-Shedding Frequency

Major efforts made in this study were to examine the variations of the instantaneous vortex-shedding frequency $f_w(t)$ in conjunction

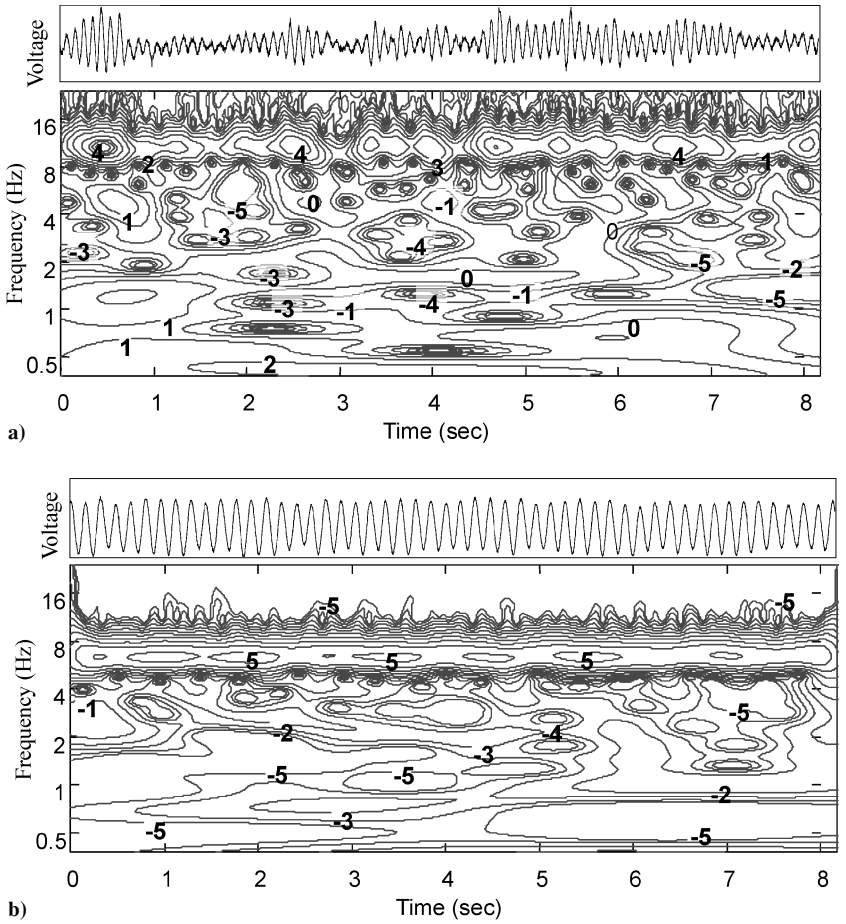

Fig. 3 Time traces and wavelet spectra of hot-wire measurements at point P4 of a) trapezoidal cylinder model and b) trapezoidal cylinder with splitter plate.

Table 1 Parameters for wavelet analysis at the Reynolds numbers studied

Reynolds number	Sampling rate, 1/s	Sampling time, s	f_s, Hz	Frequency resolution at f_s, Hz
1.8×10^3	200	20	6.0	0.029
4.1×10^3	200	20	12.1	0.060
5.2×10^3	250	16	15.1	0.061
7.7×10^3	500	8	22.0	0.044
9.8×10^3	500	8	28.8	0.057
1.6×10^4	1000	4	45.4	0.045
2.25×10^4	1000	4	63.5	0.064
2.7×10^4	1000	4	75.4	0.075

with the low-frequency modulations, $A_w(t)$. The sampling parameters were adjusted for different Reynolds numbers to ensure the relevant frequency resolution. Table 1 lists the frequency resolutions of WT at the Reynolds numbers studied, which appear to be no more than 0.5% of the corresponding mean vortex-shedding frequencies f_s.

Figure 6a shows the variations of $f_w(t)$ and $A_w(t)$ obtained at $Re = 9.8 \times 10^3$. Given that the data shown were in the discrete form, the cross correlation of $f_w(t)$ and $A_w(t)$, denoted as R_{fA}, and the cross-correlation coefficient, denoted as ρ_{fA}, are then defined as follows:

$$R_{fA}(r\,\Delta t) = \frac{1}{N-r}\sum_{n=1}^{N-r} f_n A_{n+r} \tag{3}$$

$$\rho_{fA}(r\,\Delta t) = \frac{R_{fA}(r\,\Delta t)}{\sqrt{R_{ff}(0)}\sqrt{R_{AA}(0)}} \tag{4}$$

where Δt denotes the data sampling time interval and r is an integer signifying the time lag between $f_w(t)$ and $A_w(t)$.

Consequently, Fig. 6b shows the cross-correlation coefficient of ρ_{fA} vs the time lag, in terms of τ/T_s, for $f_w(t)$ and $A_w(t)$ given in Fig. 6a. Note that T_s denotes the mean vortex-shedding period. The negative correlation at $\tau/T_s = 0$ is noted as being very significant, given that the out-of-phase characteristic between $f_w(t)$ and $A_w(t)$ can be inferred from it. Moreover, the values of $\rho_{fA}(\tau/T_s = 0)$ and the values of the most negative ρ_{fA} together with the corresponding time lag τ/T_s for all of the Reynolds numbers studied, are presented in Fig. 7. Each of the symbols shown in Figs. 7 indicates an average of 25 sets of correlation coefficients, and each of the I bars denotes the corresponding 95% confidence interval. It is shown by the solid circles in Fig. 7 that the zero time-lag cross-correlation coefficients appear to be between -0.4 and -0.5. These statistically determined negative values strongly suggest that the vortex-shedding frequency variations and the low-frequency modulations be out of phase most of the time. Namely, when the amplitude of vortex-shedding component increases the vortex-shedding frequency becomes lower, and vice versa.

In descriptions of the characteristics of the wake flow behind bluff bodies, the relations between the vortex formation length, the shedding frequency, and its amplitude are frequently mentioned in the literature. According to both previous studies and the present results, these quantities were found to be well correlated in time. A summary of these findings follows:

1) Variations of base pressure and vortex formation length are in phase essentially, based on conclusions from the previous measurements by the use of a pressure transducer and a split fiber.[24]

2) The low-frequency modulation and vortex formation length appear in phase, which can be evidenced from the simultaneous records of hot-wire signals and flow visualization obtained in the present study.

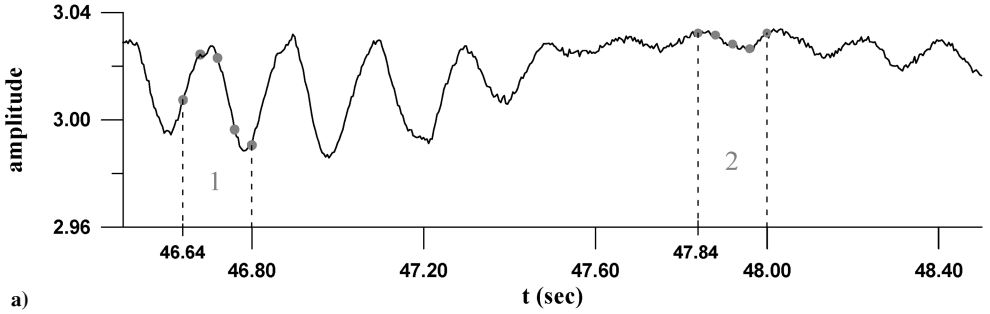

a)

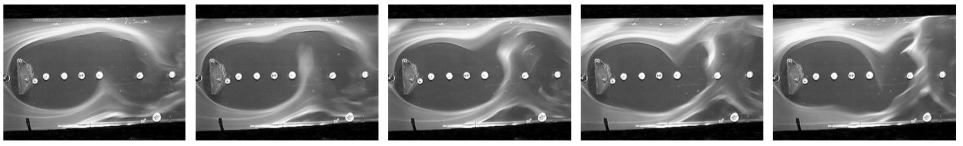

b) t = 46.64 t = 46.68 T = 46.72 t = 46.76 t = 46.80

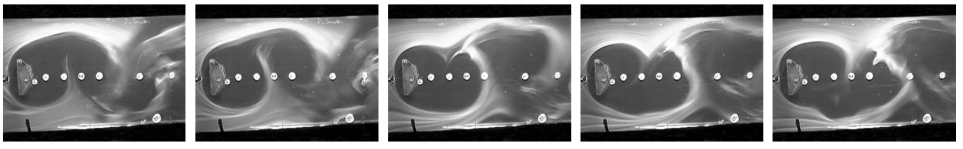

c) t = 47.84 t = 47.88 T = 47.92 t = 47.96 t = 48.00

Fig. 4 Comparison of the low-frequency modulations in the velocity fluctuations and the smoke-wire images: a) hot-wire signals measured at point P3, $Re = 1.8 \times 10^3$, b) longer formation length in time zone 1, and c) shorter formation length in time zone 2.

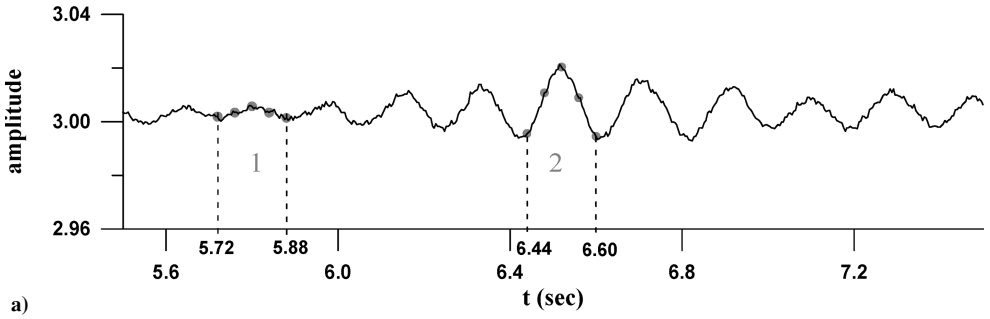

a)

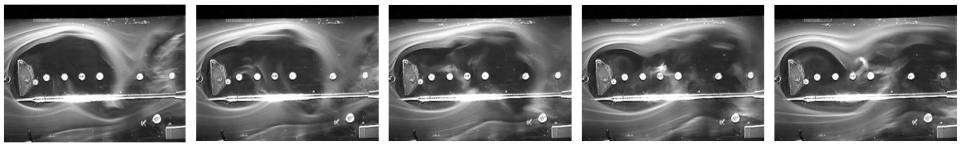

b) t = 5.64 t = 5.68 t = 5.72 t = 5.76 t = 5.80

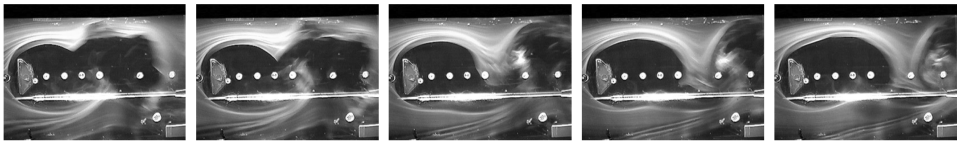

c) t = 6.44 t = 6.48 t = 6.52 t = 6.56 t = 6.60

Fig. 5 Comparison of the low-frequency modulations in the velocity fluctuations and the smoke-wire images: a) hot-wire signals measured at point P4, $Re = 1.8 \times 10^3$, b) shorter formation length in time zone 1, and c) longer formation length in time zone 2.

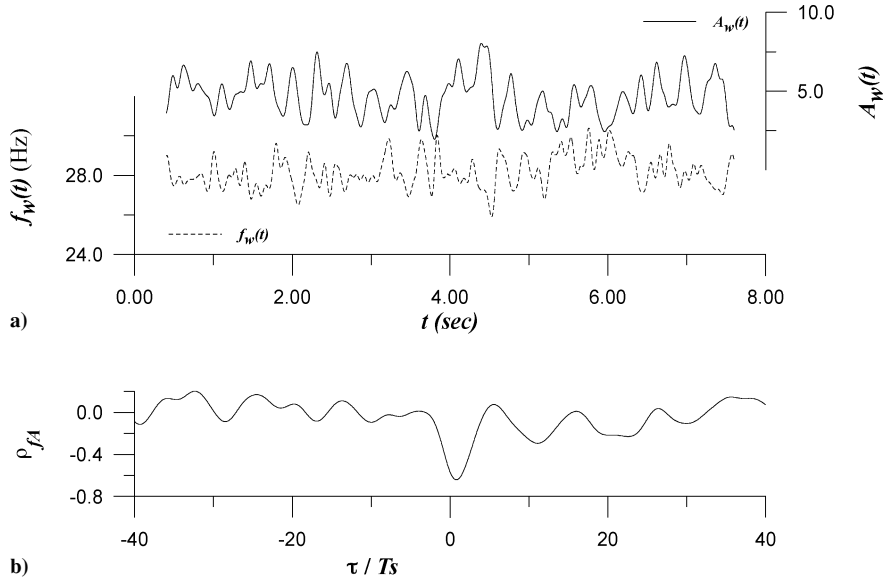

Fig. 6 Illustration of correlation between $f_w(t)$ and $A_w(t)$: a) instantaneous vortex-shedding frequency $f_w(t)$ and low-frequency modulation amplitude $A_w(t)$ extracted from the wavelet spectrum at $Re = 9.8 \times 10^3$ and b) cross-correlation coefficient of $f_w(t)$ and $A_w(t)$ in panel a.

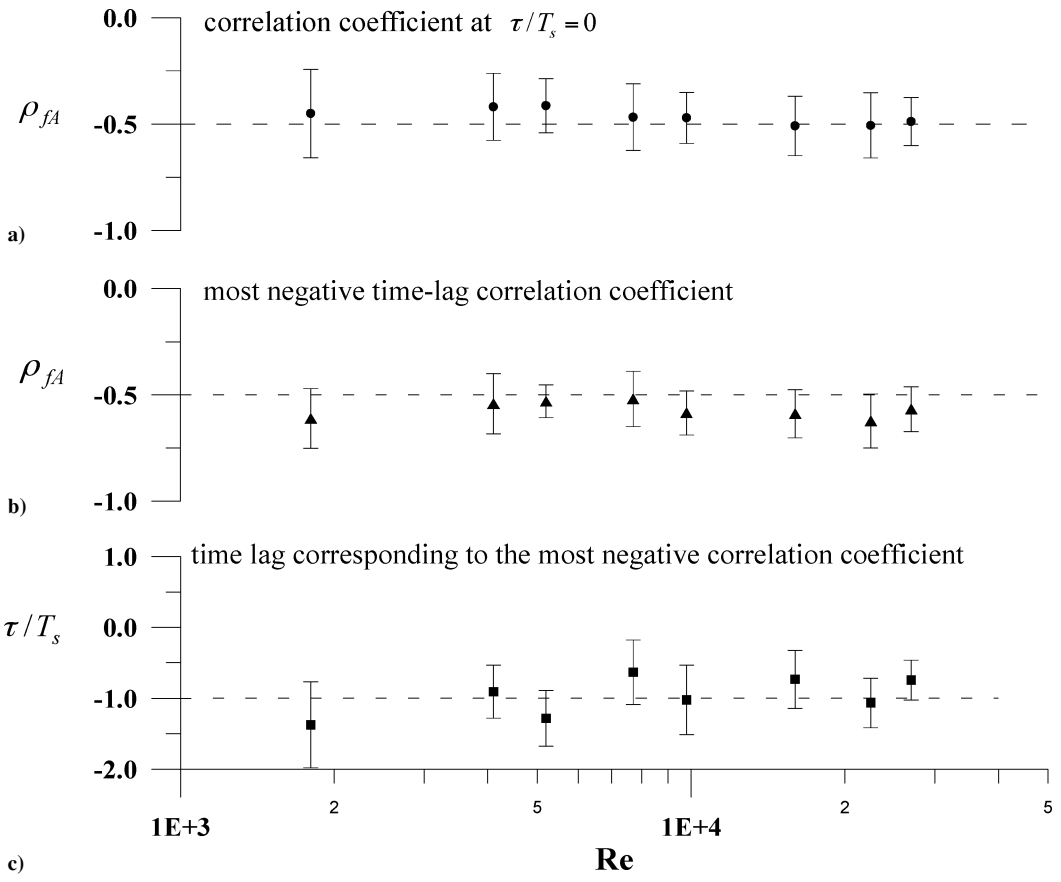

Fig. 7 Cross-correlation coefficients of $f_w(t)$ and $A_w(t)$ obtained at Reynolds numbers from 1.8×10^3 to 2.7×10^4.

3) The modulation associated with the modulus of the vortex-shedding frequency $A_w(t)$ is correlated with the instantaneous shedding frequency $f_w(t)$ in an out-of-phase manner, as evidenced by the results presented in Fig. 7.

From the preceding findings, a physical picture concerning the low-frequency modulations in the vortex-shedding process of a trapezoidal cylinder at the present Reynolds numbers emerges. First of all, the low-frequency fluctuations can be considered as associated with the flapping of the separated shear layer. As the separated shear layer moves outward, the vortex formation region is enlarged. This process entrains more fluid from the freestream and takes longer time to complete the formation of a vortical structure; thus, the amplitude of the measured signals increases and the shedding frequency decreases. In contrast, as the separated shear layer moves inward, the formation region is relatively smaller. This process entrains less fluid from the freestream and takes less time to complete the vortex formation; thus, the amplitude of the measured signals is decreased and the shedding frequency is increased.

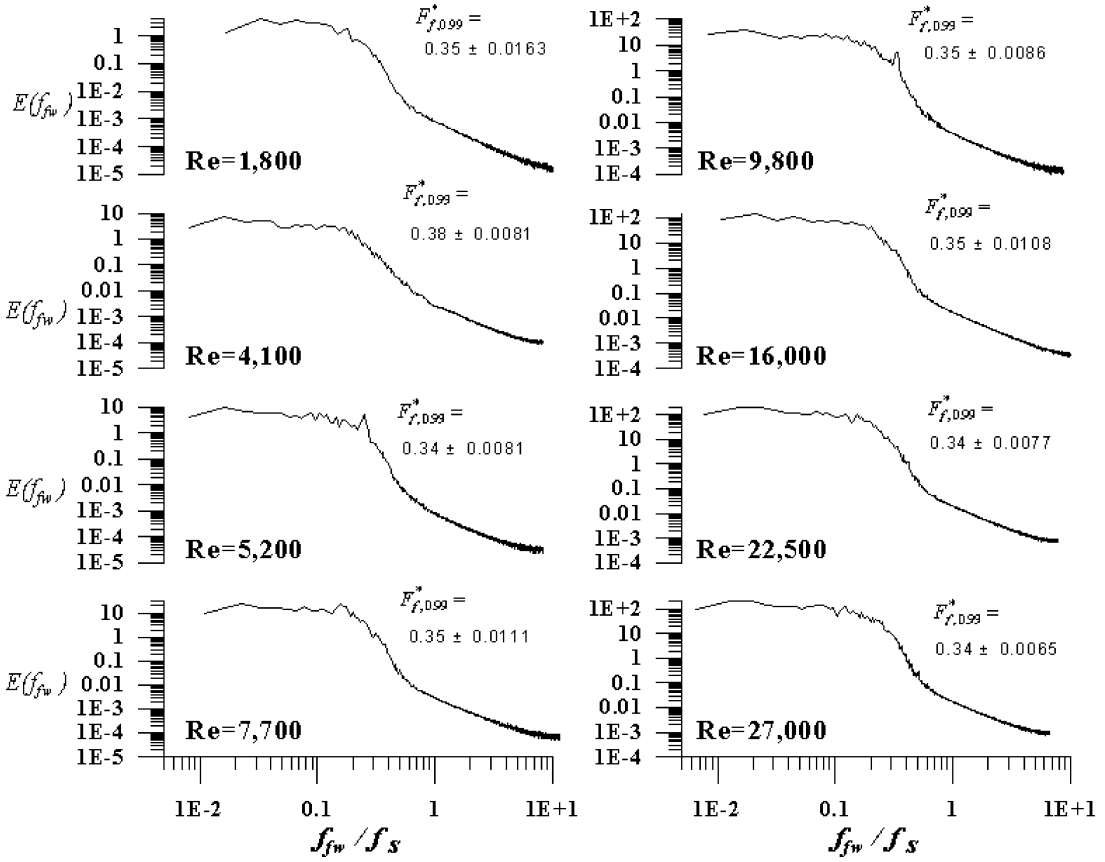

Fig. 8 FFT power spectra of $f_w(t)$ obtained at Reynolds numbers from 1.8×10^3 to 2.7×10^4.

Moreover, an interesting finding revealed from Figs. 7b and 7c is that the correlation coefficients reach the most negative values at the time lags of about one vortex-shedding period. This appearance seems to imply that the amplitude modulation is leading the variation of vortex-shedding frequency at the measured location. Further investigation on this finding is needed in the future.

C. Characteristics of Low-Frequency Modulation

Fast Fourier transform (FFT) spectral analysis was further performed on the $f_w(t)$ curves obtained in this study. The spectra results are shown in Fig. 8. In each of the spectra, the horizontal axis is expressed with a nondimensional parameter:

$$F_f^* = f_{fw}/f_s \tag{5}$$

where f_{fw} and f_s denote the frequency associated with the variations of $f_w(t)$and the mean vortex-shedding frequency, respectively. All of the spectra shown in Fig. 8 reveal a feature in common that the values of $E(f_{fw})$ in the frequency range of $F_f^* < 0.1$ are predominant, which implies that the variations of $f_w(t)$ are characterized by the frequencies of one order smaller than the vortex-shedding frequency. These appearances substantiate the previous observations concerning the characteristic behavior of low-frequency modulations.[6,16,20] To be more specific regarding this flow characteristic, a parameter,$F^*_{f,0.99}$, is defined as follows:

$$\frac{\int_0^{F^*_{f,0.99}} E(f_{fw})\,\mathrm{d}F_f^*}{\int_0^{\infty} E(f_{fw})\,\mathrm{d}F_f^*} = 0.99 \tag{6}$$

In Eq. (6), $F^*_{f,0.99}$ denotes the frequency below which the spectral energy content is accumulated to 99% of the total. As seen in Fig. 8, the values of $F^*_{f,0.99}$ obtained at the Reynolds numbers studied are about 0.35.

Similarly, one can examine the characteristics of $A_w(t)$ with the parameters F_A^* and $F^*_{A,0.99}$, defined as

$$F_A^* = \frac{f_{Aw}}{f_s} \tag{7}$$

$$\frac{\int_0^{F^*_{A,0.99}} E(f_{Aw})\,\mathrm{d}F_A^*}{\int_0^{\infty} E(f_{Aw})\,\mathrm{d}F_A^*} = 0.99 \tag{8}$$

The spectral distributions of $A_w(t)$, that is, $E(f_{Aw})$ vs F_A^*, and the corresponding values of $F^*_{A,0.99}$, are shown in Fig. 9. The curves of $E(f_{Aw})$ corresponding to different Reynolds numbers studied also show a feature in common, namely, that a pronounced transition takes place at F_A^* between 0.1 and 1, which bear the similarity to the appearances of $E(f_{fw})$ shown in Fig. 8. Also note that the values of$F^*_{A,0.99}$ shown in Fig. 9 are around 0.27, somewhat less than those of $F^*_{f,0.99}$ given in Fig. 8. Generally speaking, the spectral curves presented in Figs. 8 and 9 confirm that the variations of $f_w(t)$ and $A_w(t)$ are characterized by the frequencies much lower than the vortex-shedding frequency.

The characteristics of $A_w(t)$ and $f_w(t)$ can be further examined with the following expressions:

$$\sigma_f^* = \sigma_f/\overline{f_w(t)} \tag{9}$$

$$\sigma_A^* = \sigma_A/\overline{A_w(t)} \tag{10}$$

where σ_f and σ_A denote the standard deviations of $f_w(t)$and$A_w(t)$, respectively, and the upper bars denotes the time mean values. Basically, one can say that σ_f^* and σ_A^* represent the fluctuation levels of $f_w(t)$ and $A_w(t)$, respectively.

Figure 10a shows that the σ_f^* values are about 2.5% for all of the Reynolds numbers studied. This quantitative characteristic is noted to be in good agreement with the observation reported by Blevins.[22] Because the frequency resolution of the present wavelet

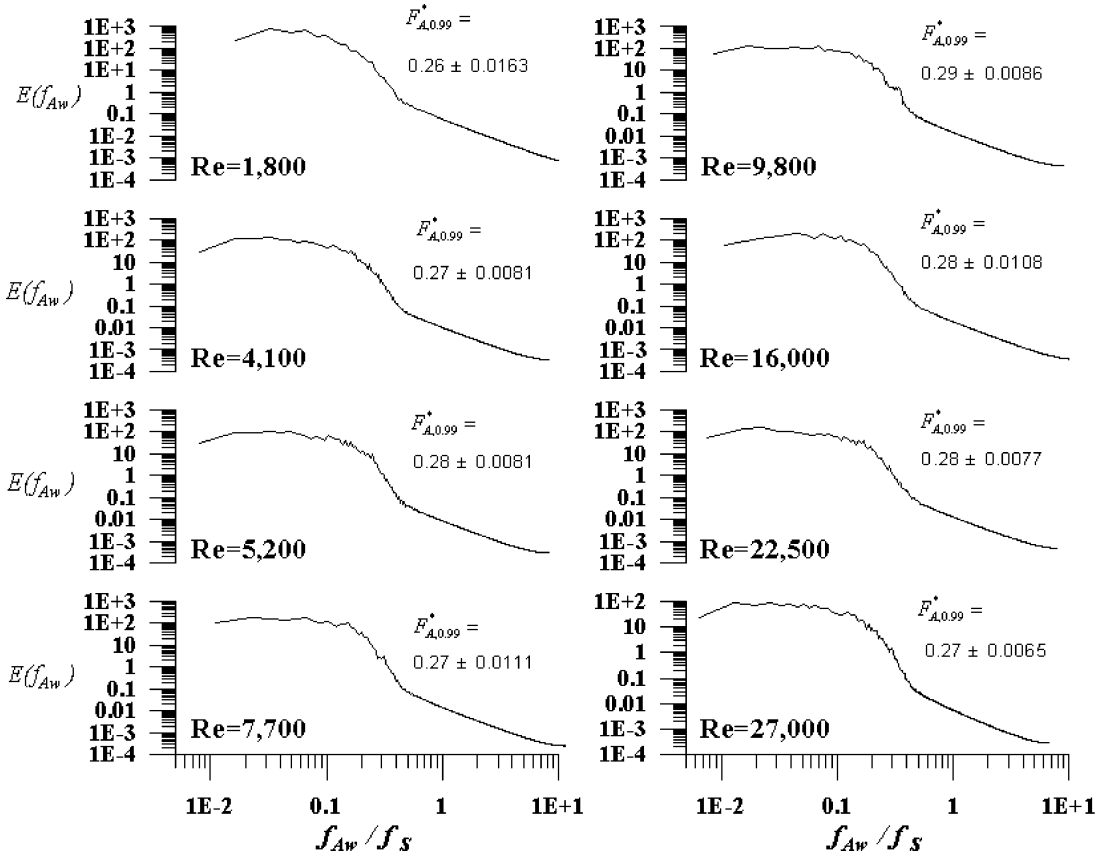

Fig. 9 FFT power spectra of $A_w(t)$ obtained at Reynolds numbers from 1.8×10^3 to 2.7×10^4.

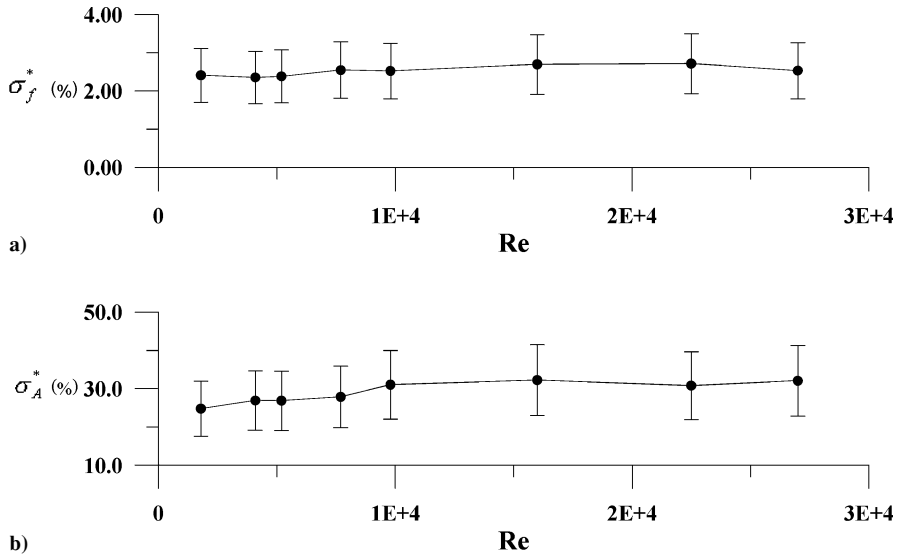

Fig. 10 Variation of a) σ_f^* and b) σ_A^* vs *Re*.

analysis is better than 0.5% of the mean vortex shedding frequency, as seen in Table 1, the σ_f^* values shown in Fig. 10a are physically meaningful. On the other hand, in Fig. 10b, the distribution of σ_A^* vs Reynolds numbers shows that the σ_A^* values increase from 25 to 30% for Reynolds numbers from 10^3 to 10^4.

D. Integral Timescale of Low-Frequency Modulation

The integral timescale I_t of $A_w(t)$ can be expressed as follows:

$$I_t = \int_0^{\tau_c} \rho_{AA}\, \mathrm{d}\tau \tag{11}$$

where ρ_{AA} is actually reduced from ensemble averaging over 25 sets of the autocorrelation curves of $A_w(t)$, and τ_c denotes the first zero crossing of ρ_{AA} on the τ axis, where τ denotes the time delay in the autocorrelation. I_t indicates a measure of the time interval over which a fluctuating quantity is correlated with itself, or, equivalently speaking, a time measure over which the quantity is dependent on its past values.[39]

As seen in Fig. 11, I_t decays with the Reynolds numbers studied. The trend can be indicated by a numerical curve. If one further normalizes each of the I_t values by T_s, the results of different Reynolds numbers appear to be about a constant value 2. In analyzing the low-frequency modulations of the present wake flow configuration,

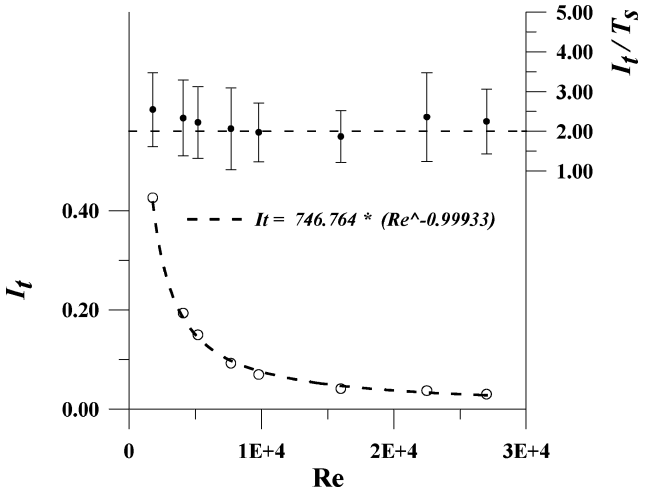

Fig. 11 I_t **and** I_t/T_s **vs Reynolds number.**

Miau et al.[21] employed a low-pass filter for processing the measured base pressure signals and found that the integral timescale associated with the low-frequency modulations is about two times the vortex-shedding period. Although the quantity measured and the data reduction technique employed in the present study are different from those reported by Miau et al.,[21] the findings of these two studies in this regard are in very good agreement. Thus, it is fair to say that the integral timescale of the low-frequency modulations is about two times the vortex-shedding period.

V. Conclusions

In this study, the relation between the low-frequency modulations and the vortex formation length was examined first, in accordance with the hot-wire measurement and the smoke-wire flow visualization obtained simultaneously. Second, the relation between low-frequency modulations and instantaneous vortex-shedding frequency was investigated by the use of the wavelet analysis and a cross-correlation technique. Subsequently, the characteristic behavior of low-frequency modulations was described in terms of the integral timescale deduced.

The experiments were conducted at Reynolds numbers in a range between 1.8×10^3 and 2.7×10^4. Major findings can be summarized as follows:

1) The low-frequency modulations in the vortex-shedding process are associated with the separation region behind the bluff body swollen and shrunk in time. This is substantiated by the simultaneous smoke-wire images and the hot-wire signals measured.

2) The low-frequency modulation and the instantaneous vortex-shedding frequency reduced are well correlated, as indicated by the obtained negative correlation coefficient up to -0.5. Namely, the larger the vortex formation length, the lower the vortex-shedding frequency, and vice versa.

3) The undulation associated with the low-frequency modulations, expressed in terms of a normalized quality $A*$, shows a growth from 25 to 30% for the Reynolds numbers increased from 1.8×10^3 to 2.7×10^4. This infers that the low-frequency modulations become significant as the Reynolds numbers get higher. On the other hand, the variations of vortex-shedding frequency are about 2.5% of the mean value, for all of the Reynolds numbers studied.

4) The integral timescale of the low-frequency modulations is found to be about two times the time-mean vortex-shedding period, which is in very good agreement with previous findings.

Acknowledgments

The authors acknowledge the support by the National Science Council, Republic of China, for this research under Contract NSC 90-2212-E-006-153. The wavelet transform program by C. Torrence and G. Compo, available at URL: http://paos.colorado.edu/research/wavelets/, is gratefully acknowledged.

References

[1]Roshko, A., "On the Development of Turbulent Wakes from Vortex Streets," NACA Rept. 1191, 1954.

[2]Tritton, D. J., "Experiments on the Flow past a Circular Cylinder at Low Reynolds Number," *Journal of Fluid Mechanics*, Vol. 16, 1959, pp. 547–567.

[3]Bloor, M. S., "The Transition to Turbulence in the Wake of a Circular Cylinder," *Journal of Fluid Mechanics*, Vol. 19, 1964, pp. 290–304.

[4]Gerrard, J. H., "The Three-Dimensional Structure of the Wake of a Circular Cylinder," *Journal of Fluid Mechanics*, Vol. 25, Pt. 1, 1966, pp. 143–164.

[5]Hanson, F. B., and Richardson, P. D., "The Near-Wake of a Circular Cylinder in Crossflow," *Journal of Basic Engineering*, Vol. 90, 1968, pp. 476–484.

[6]Roshko, A., "Perspectives on Bluff Body Aerodynamics," *Journal of Wind Engineering and Industrial Aerodynamics*, Vol. 49, 1993, pp. 79–100.

[7]Graham, J. M. R., "The Effect of End-Plates on Two-Dimensionality of a Vortex Wake," *Aeronautical Quarterly*, Vol. 20, 1969, pp. 237–247.

[8]Fox, T. A., and West, G. S., "On the Use of End Plates with Circular Cylinders," *Experiments in Fluids*, Vol. 9, 1990, pp. 231–239.

[9]Szepessy, S., and Bearman, P. W., "Aspect Ratio and End Plate Effects on Vortex Shedding from a Circular Cylinder," *Journal of Fluid Mechanics*, Vol. 234, 1992, pp. 191–217.

[10]Norberg, C., "An Experimental Investigation of the Flow Around a Circular Cylinder: Influence of Aspect Ratio," *Journal of Fluid Mechanics*, Vol. 258, 1994, pp. 287–316.

[11]Stansby, P. K., "The Effects of End Plates on the Base Pressure Coefficients of a Circular Cylinder," *Aeronautical Journal*, Vol. 78, 1974, pp. 36, 37.

[12]Gerich, D., and Eckelmann, H., "Influence of End Plates and Free Ends on the Shedding Frequency of Circular Cylinders," *Journal of Fluid Mechanics*, Vol. 122, 1982, pp. 109–121.

[13]Stäger, R., and Eckelmann, H., "The Effect of Endplates on the Shedding Frequency of a Circular Cylinders in the Irregular Range," *Physics of Fluids A*, Vol. 3, No. 9, 1991, pp. 2116–2121.

[14]Williamson, C. H. K., "The Natural and Forced Formation of Spot-Like 'Vortex Dislocations' in the Transition of a Wake," *Journal of Fluid Mechanics*, Vol. 243, 1992, pp. 393–441.

[15]Williamson, C. H. K., "Vortex Dynamics in the Cylinder Wake," *Annual Review of Fluid Mechanics*, Vol. 28, 1996, pp. 477–539.

[16]Yang, P.-M., Hussein, M., and Williams, D. R., "Oblique and Parallel Wave Interaction in the Near Wake of a Circular Cylinder," *Physics of Fluids A*, Vol. 5, No. 7, 1993, pp. 1657–1661.

[17]Blackburn, H. M., and Melbourne, W. H., "The Effect of Free-Stream Turbulence on Sectional Lift Forces on a Circular Cylinder," *Journal of Fluid Mechanics*, Vol. 306, 1996, pp. 267–292.

[18]Henderson, R. C., "Nonlinear Dynamics and Pattern Formation in Turbulent Wake Transition," *Journal of Fluid Mechanics*, Vol. 352, 1997, pp. 65–112.

[19]Najjar, F. M., and Balachandar, S., "Low-Frequency Unsteadiness in the Wake of a Normal Flat Plate," *Journal of Fluid Mechanics*, Vol. 370, 1998, pp. 101–147.

[20]Lisoski, D., "Nominally 2-Dimensional Flow About a Normal Flat Plate," Ph.D. Dissertation, Graduate Aeronautical Labs., California Inst. of Technology, Pasadena, CA, Aug. 1993.

[21]Miau, J. J., Wang, J. T., Chou, J. H., and Wei, C. Y., "Low-Frequency Fluctuations in the Near Wake Region of a Trapezoidal Cylinder with Low Aspect Ratio," *Journal of Fluids and Structures*, Vol. 17, 2003, pp. 701–715.

[22]Blevins, R. D., "The Effect of Sound on Vortex Shedding from Cylinders," *Journal of Fluid Mechanics*, Vol. 161, 1985, pp. 217–237.

[23]Miau, J. J., Yang, C. C., Chou, J. H., and Lee, K. R., "Suppression of Low-Frequency Variations in Vortex Shedding by a Splitter Plate Behind a Bluff Body," *Journal of Fluids and Structures*, Vol. 7, 1993, pp. 897–912.

[24]Miau, J. J., Wang, J. T., Chou, J. H., and Wei, C. Y., "Characteristics of Low-Frequency Variations Embedded in Vortex Shedding Process," *Journal of Fluids and Structures*, Vol. 13, 1999, pp. 339–359.

[25]Grossman, A., and Morlet, J., "Decomposition of Hardy Functions into Square Integrable Wavelets of Constant Shape," *SIAM Journal on Mathematical Analysis*, Vol. 15, No. 4, 1984, pp. 723–736.

[26]Kiya, M., and Abe, Y., "Turbulent Elliptic Wakes," *Journal Fluids and Structures*, Vol. 13, 1999, pp. 1041–1067.

[27]Lewis, C. G., and Gharib, M., "An Exploration of the Wake Three Dimensionalities Caused by a Local Discontinuity in Cylinder Diameter," *Physics of Fluids A*, Vol. 4, 1992, pp. 104–117.

[28]Hangan, H., Kopp, G. A., Vernet, A., and Martinuzzi, R., "A Wavelet Pattern Recognition Technique for Identifying Flow Structures in Cylinder Generated Wakes," *Journal of Wind Engineering and Industrial Aerodynamics*, Vol. 89, 2001, pp. 1001–1015.

[29]Higuchi, H., Lewalle, J., and Crane, P., "On the Structure of a Two-Dimensional Wake Behind a Pair of Flat Plates," *Physics of Fluids*, Vol. 6, 1994, pp. 297–305.

[30]Braza, M., Faghani, D., and Persillon, H., "Successive Stages and the Role of Natural Vortex Dislocations in Three-Dimensional Wake Transition," *Journal of Fluid Mechanics*, 2001, Vol. 439, pp. 1–41.

[31]Farge, M., "Wavelet Transforms and Their Applications to Turbulence," *Annual Review of Fluid Mechanics*, Vol. 24, 1992, pp. 395–457.

[32]Bendat, J. S., and Piersol, A. G., *Random Data: Analysis and Measurement Procedures*, 2nd ed., Wiley, New York, 1986, Chap. 13.

[33]Hu, C. C., Miau, J. J., and Chou, J. H., "Instantaneous Vortex-Shedding Behaviour in Periodically Varying Flow," *Proceedings of the Royal Society of London, Series A: Mathematical and Physical Sciences*, Vol. 458, 2001, pp. 911–932.

[34]Huang, N. E., Shen, Z., Long, S. R., Wu, M. C., Shih, H. H., Zheng, Q., Yen, N. C., Tung, C. C., and Liu, H. H., "The Empirical Mode Decomposition and the Hilbert Spectrum for Nonlinear and Non-Stationary Time Series Analysis," *Proceedings of the Royal Society of London, Series A: Mathematical and Physical Sciences*, Vol. 454, 1998, pp. 903–995.

[35]Ishikawa, H., Kiya, M., Komaki, Y., and Mochizuki, O., "Low-Frequency Modulation of Turbulent Karman Vortex Street," *Transactions of the Japan Society of Mechanical Engineers B*, Vol. 62, 1996, pp. 2180–2186.

[36]Hamdan, N. N., Jurban, B. A., Shabaneh, N. H., and Abu-Samak, M., "Comparison of Various Basic Wavelets for the Analysis of Flow-Induced Vibration of a Cylinder in Cross Flow," *Journal of Fluids and Structures*, Vol. 10, 1996, pp. 633–651.

[37]Torrence, C., and Compo, G. P., "A Practical Guide to Wavelet Analysis," *Bulletin of the American Meteorological Society*, Vol. 79, 1998, pp. 61–78.

[38]Carmona, R. A., Hwang, W. L., and Torrésani, B., "Characterization of Signals by the Ridges of Their Wavelet Transform," *IEEE Transactions on Signal Processing*, Vol. 45, 1997, pp. 2586–2590.

[39]Tennekes, H., and Lumley J. L., *A First Course in Turbulence*, MIT Press, Cambridge, MA, 1972, Chap. 6.

K. Ghia
Associate Editor